Rational W-shaped solitons on a continuous-wave background in the Sasa-Satsuma equation

Li-Chen Zhao,[1] Sheng-Chang Li,[2,*] and Liming Ling[3,†]
[1]*Department of Physics, Northwest University, Xi'an 710069, China*
[2]*School of Science, Xi'an Jiaotong University, Xi'an 710049, China*
[3]*Department of Mathematics, South China University of Technology, Guangzhou 510640, China*
(Received 13 November 2013; revised manuscript received 27 January 2014; published 28 February 2014)

We investigate the solution in rational form for the Sasa-Satsuma equation on a continuous background which describes a nonlinear fiber system with higher-order effects including the third-order dispersion, Kerr dispersion, and stimulated inelastic scattering. The W-shaped soliton in the system is obtained analytically. It is found that the height of hump for the soliton increases with decreasing the background frequency in certain parameter regime. The maximum height of the soliton can be three times the background's height and the corresponding profile is identical with the one for the well-known eye-shaped rogue wave with maximum peak. The numerical simulations indicate that the W-shaped soliton is stable with small perturbations. Particularly, we show that the W-shaped soliton corresponds to a stable supercontinuum pulse by performing exact spectrum analysis.

DOI: 10.1103/PhysRevE.89.023210 PACS number(s): 42.65.Tg, 05.45.Yv, 42.81.Dp

I. INTRODUCTION

Recently, Kuanetsov-Ma solitons, Akhmediev breathers, and Peregrine rogue waves (rw) have been observed in nonlinear fiber [1–3], which provides a good platform to study the dynamics of nonlinear localized waves on a continuous-wave (cw) background conveniently. These experimental studies showed that the simplified nonlinear Schrödinger (NLS) equation can well describe the dynamics of localized waves, which only contains the group velocity dispersion (GVD) and its counterpart, namely, self-phase modulation (SPM). However, for ultrashort pulses whose duration is shorter than 100 fs, which is tempting and desirable to improve the capacity of high-bit-rate transmission systems, the nonlinear susceptibility will produce higher-order nonlinear effects like the Kerr dispersion (i.e., self-steepening) and the stimulated Raman scattering (SRS) except for SPM. Apart from GVD, the ultrashort pulses will also suffer from the third-order dispersion (TOD). These are the most general terms that have to be taken into account when extending the applicability of the NLS equation [4,5]. With these effects, the corresponding integrable equation was derived as the Sasa-Satsuma (S-S) equation [6].

The investigations on the S-S equation indicated that the nonlinear waves in nonlinear fiber with the high-order effects are much more diverse than the ones in a simplified NLS equation [6–11]. Very recently, it was found that the high-order effects could make the rw twisted and the rational solution of the S-S equation had distinctive properties in contrast to that of the well-known NLS equation [12,13]. The linearized stability analysis for the S-S equation in Ref. [7] suggested that there are both modulational instability and stability regimes for low perturbation frequencies on the cw background. The rational solutions obtained in Refs. [12,13] are all in the modulational instability regime. Then we expect that the soliton solution could exist on the cw background in the modulational stability regime.

In this paper, we study the analytical rational solution on cw background in the S-S equation through the Darboux transformation method. In contrast to the rational solutions in the simplified NLS equation, which have been used to describe rw phenomena photographically [14–17], we present an exact rational solution in explicit form which corresponds to the W-shaped soliton. Furthermore, we discuss the stability properties of the rational W-shaped soliton and the numerical stimulations show that the soliton is stable. We perform the spectrum analysis on the W-shaped soliton, Peregrine rw, and the rw with two humps obtained in Refs. [12,13]. The spectrum comparison suggests that the W-shaped soliton corresponds to a stable supercontinuum pulse in the frequency domain.

II. S-S EQUATION AND W-SHAPED SOLITON ON CW BACKGROUND

According to the original work of Sasa and Satsuma [6], the evolution equation for the optical fields in a nonlinear fiber with the high-order effects mentioned above can be written as

$$iE_z + \tfrac{1}{2}E_{tt} + |E|^2E + i\epsilon(E_{ttt} + 6|E|^2E_t + 3E|E|^2_t) = 0, \tag{1}$$

where E is the amplitude of the slowly varying envelope of the optical field; t and z are the retarded time and propagation distance, respectively. Here the real parameter ϵ is introduced to describe the integrable perturbations in the NLS equation. The units are dimensionless after performing proper scalar transformation. When $\epsilon = 0$, Eq. (1) reduces to the standard NLS equation which only has the terms describing the lowest-order dispersion and SPM. The soliton solutions of Eq. (1) have been presented on the zero background in Refs. [18–20]. Now we study the rational solutions on a cw background, i.e.,

$$E_0(t,z) = c\exp[i\omega_0 t + iK(z)], \tag{2}$$

with

$$K(z) = -\frac{\omega_1}{12\epsilon}z + \epsilon\omega_1^3 z - 6\epsilon\omega_1 c^2 z - \frac{z}{108\epsilon^2},$$

where $\omega_1 = \omega_0 - \frac{1}{6\epsilon}$. The parameter c denotes the background amplitude. ω_0 is the frequency of the optical background field. By performing the Darboux transformation [21] from the above seed solution, one can derive the kinds of localized

*scli@mail.xjtu.edu.cn
†lingliming@qq.com

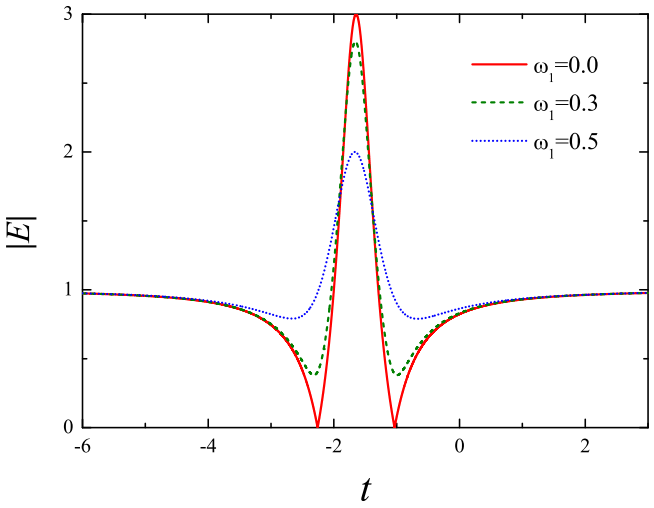

FIG. 1. (Color online) The profiles of the rational solution $|E(t,z)|$ at $z=0$ with $\omega_1=0$ (red solid line), $\omega_1=0.3$ (green dashed line), and $\omega_1=0.5$ (blue dotted line). It is seen that the height of the hump is inversely proportional to the background frequency in the regime $0\leqslant\omega_1\leqslant\frac{c}{2}$. The parameters are $c=1$ and $\epsilon=0.1$.

waves solution. Notably, we find a new type rational solution on continuous background with some conditions on the background's amplitude and frequency, i.e., $0\leqslant\omega_1\leqslant\frac{c}{2}$. The explicit form of the rational solution is given in the Appendix.

It should be emphasized that the rational solution obtained here does not correspond to the rw in the simplified NLS equation [1,22–24]. The reason is that our solution shares common dynamical properties with a soliton which maintains its profile during the evolution. In Fig. 1 we show the profiles of the rational solution which looks like a "W", including one hump and two valleys. The similar W-shaped soliton in nonrational form has been obtained in the S-S equation [8] and in other equations which can be derived from the two-dimensional Euler equation by using the approximation procedure [25]. From Fig. 1, we see that the height of the W-shaped soliton's hump and the depth of the valleys strongly depend on the cw background's frequency ω_0. The hump's height increases as ω_1 decreases in the regime $0\leqslant\omega_1\leqslant\frac{c}{2}$. The minimum height of the hump can be two times that of the background when $\omega_1=\frac{c}{2}$ and the maximum height can be three times that of the background when $\omega_1=0$. These properties can maintain with arbitrary nonzero parameter c.

It is noted that our rational W-shaped soliton is different from the W-shaped soliton obtained in Ref. [8] (e.g., both the heights of humps and the depths of valleys are different). For the S-S equation, the linearized stability analysis in Ref. [7] suggested that there are both modulational instability and stability regimes for low perturbation frequencies on a cw background. This result is quite different from that for the simplified NLS equation where there is only an instability regime with low perturbation frequencies on the cw background. In general, the rational solution can be written as a signal part plus the cw background part. If the signal can be understood as the perturbation in the modulation instability regime, then it will be amplified exponentially and oscillating, which can induce rw dynamics [1,2]. If the signal can be understood as the perturbation in the modulation stability regime, it will not be amplified exponentially and thus it is stable. Based on these results, we can qualitatively know that the rational solutions reported in Ref. [12,13] are in the modulational instability regime since the solutions' dynamics corresponds to the rw behavior. However, the rational solution obtained here should be in the modulational stability regime [7]. We verify this statement by performing numerical simulations in Sec. IV.

III. TWO EXPLICIT CASES FOR THE RATIONAL W-SHAPED SOLITON SOLUTION

In fact, the generalized rational W-shaped soliton solution is very complicated in the regime $0\leqslant\omega_1\leqslant\frac{c}{2}$. To demonstrate the main properties of the W-shaped soliton more clearly, in this section we only discuss the properties of the W-shaped soliton in two limit cases corresponding to the situations that the height of the hump takes maximum and minimum values, respectively.

Case 1. When $\omega_1=0$ and $c=1$, the generalized rational solution can reduce to

$$E(t,z)=\left[\frac{2}{4T^2-2T(48z\epsilon+\sqrt{2}-4)+576z^2\epsilon^2+24(\sqrt{2}-4)z\epsilon-2\sqrt{2}+5}-1\right]\exp\left[\frac{i}{6\epsilon}\left(t-\frac{z}{18\epsilon}\right)\right],\tag{3}$$

where $T=t-\frac{z}{12\epsilon}$. In this case, the height of the hump of the soliton can be maximum. In Fig. 2(a), we plot the analytical solution in (t,z) plane. It is seen that the whole structure with two valleys and one hump well maintain during all propagation distance. The fact implies that the solution behaves like a soliton solution although it takes the rational solution form. This behavior is quite different from the rational solution for the same model presented in Refs. [12,13]. The profile of the soliton in this case is similar to the W-shaped soliton presented in Ref. [8]. However, we find that the middle hump is much higher than the background and its $|E|^2$ value is nine times the background's height, which is distinctive from the soliton in Ref. [8]. Moreover, it is shown that the minimum of the hump density is nearly zero (see the red solid line in Fig. 1) and the profile of our soliton is identical with the well-known fundamental rw solution for the highest peak case in the simplified NLS equation [1,22–24].

Case 2. When $\omega_1=\frac{c}{2}$ and $c=1$, the exact rational solution can be simplified as

$$E(t,z)=\left\{\frac{i\sqrt{3}-1}{2}+\frac{2[-99(\sqrt{3}+i)\epsilon z+12(\sqrt{3}+i)T+(-3+\sqrt{3}+2\sqrt{3}i)(8-8i)]}{-3267\epsilon^2z^2+8T[99\epsilon z+4(\sqrt{3}-6)]-264(\sqrt{3}-6)\epsilon z-48T^2+32(2\sqrt{3}-7)}\right\}$$
$$\times\exp\left[\frac{i}{6\epsilon}\left(t-\frac{z}{18\epsilon}\right)+\frac{1}{8}i(4T-23z\epsilon)\right].\tag{4}$$

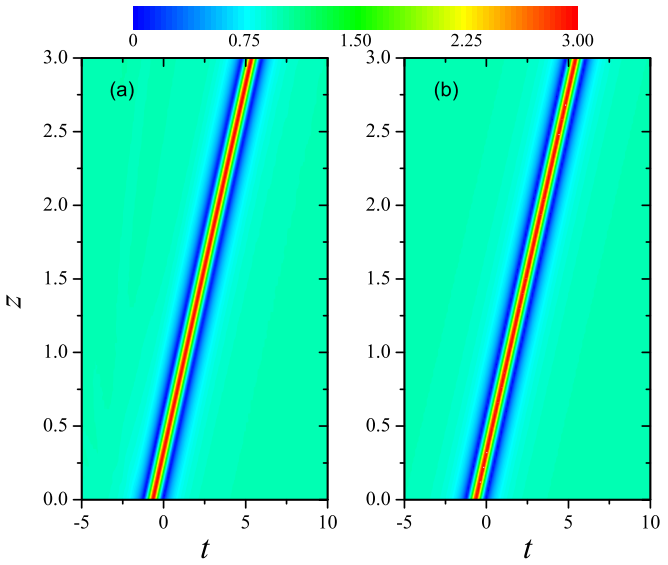

FIG. 2. (Color online) (a) The evolution of the rational solution $|E(t,z)|$ given in Eq. (3) with $\epsilon = 0.1$. (b) The corresponding numerical results for the evolution process from $E(t,0)$ with a small perturbation set as $0.02\sin(0.05t)$.

In this case, it is found that the evolution of the rational solution is similar to the situation in case 1, as shown in Fig. 2(a). However, the profile of the soliton is different from that in case 1, which can be seen from Fig. 1 (see the blue dotted line and red solid line). To demonstrate the difference between the two limit cases clearly, we calculate the the quantity $|E|^2$ in case 2 for the hump $|E|^2 = 4$ while for the valleys $|E|^2 = \frac{5}{8}$. These properties indicate that the structure characters are independent of the perturbation parameter ϵ. For both two cases, the traveling trajectories of the solitons are straight lines in the temporal-spatial distribution plane. The trajectory is determined by the relation $\frac{\partial t}{\partial z} = \frac{99\epsilon^2+1}{12\epsilon}$. This implies that the parameter ϵ determines the traveling trajectory of the soliton, which suggests that these higher-order effects can modify the propagating speed of the solitons in the S-S model. This result holds for all W-shaped solitons obtained above.

IV. STABILITY AND SPECTRUM ANALYSIS FOR THE W-SHAPED SOLITON

The stability is much important to the solution in a nonlinear equation, now we discuss this issue for the W-shaped soliton. For simplicity, we fix the parameters c and ω_1. Under this condition, we directly perform a numerical evolution from the initial pulse $E(t,0)$ with some small perturbations by adopting the split-step Fourier method. As an example, we study the stability properties of the steepest W-shaped soliton corresponding to the rational solution in case 1. The numerical results are plotted in Fig. 2(b). For comparison, we also show the analytical results in Fig. 2(a). It is found that the numerical evolution results with the small perturbation $0.02\sin 0.05t$ are consistent with the analytical ones. Moreover, we compare the profiles at different propagation distances in Fig. 3. It is shown that the profiles of the exact and numerical solutions are very consistent except for some slight deviations. These results

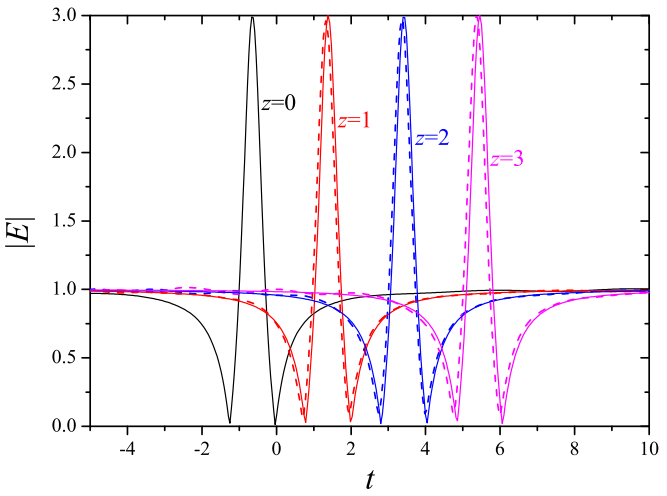

FIG. 3. (Color online) The profiles of the W-shaped soliton in case 1 at $z = 0,1,2,3$. The solid lines denote the analytical solutions while the dashed lines correspond to the numerical results.

suggest that our soliton solution is stable. To further check this point, we make wide simulations by scanning a considerable portion of the parameters space. In the simulations we set the small perturbation as $0.02\sin(\Omega t)$ and then vary the modulation frequency Ω and change the parameter ϵ. Finally, we estimate the deviations for both the maximum [see Fig. 4(a)] and the minimum [see Fig. 4(b)] values of $|E|$ between the analytical and numerical results. From Fig. 4, we find that the maximum deviations after propagating three units is much smaller than the initial perturbation in a wide range of the parameter plane (Ω,ϵ). All simulation results indicate that

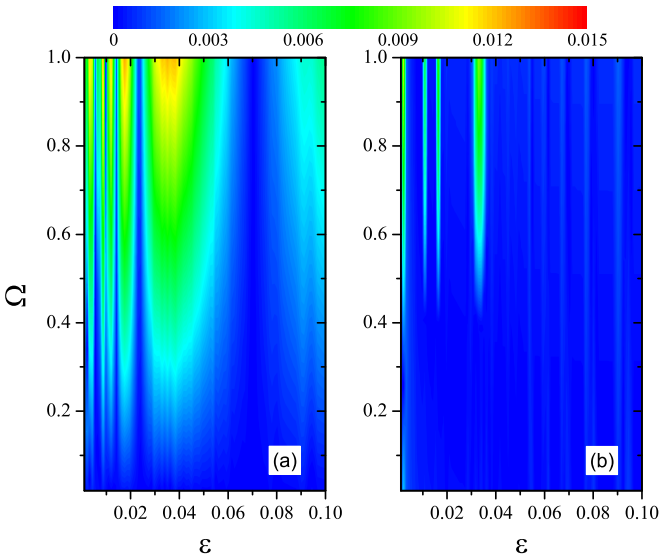

FIG. 4. (Color online) (a) The differences between the numerical and analytical results for the maximum values of $|E|$ in the parameter plane (ϵ,Ω) at $z = 3$. (b) The corresponding differences for the minimum values of $|E|$. The numerical results are obtained by evolving $E(t,0)$ [given by Eq. (3)] with a small perturbation $0.02\sin\Omega t$.

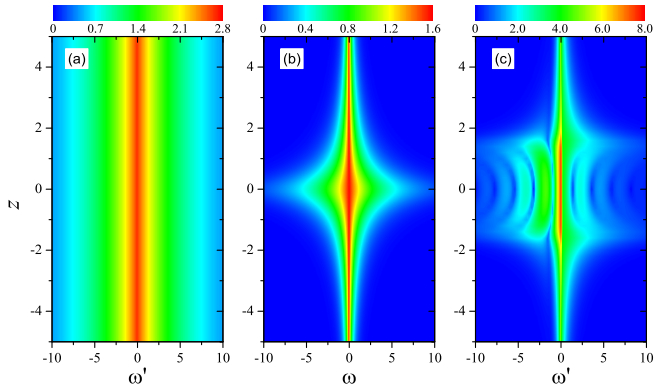

FIG. 5. (Color online) (a) The spectrum evolution [i.e., $\sqrt{|F(\omega,z)|}$] of the rational solution in case 1 with $\omega_1 = 0$. The parameters are $c = 1$ and $\epsilon = 0.1$. (b) The spectrum evolution [i.e., $\sqrt{|F_1(\omega,z)|}$] of a Peregrine rw. (c) The spectrum evolution [i.e., $\sqrt{|F_p(\omega,z)|}$] of the rw pair of S-S model (corresponding to the rws in Fig. 2 in Ref. [13]).

the W-shaped soliton is stable under small perturbations and low modulation frequencies.

The studies on modulational instability induced supercontinuum generation indicated that the rw excitation is related with supercontinuum generation in an optical fiber [2,26,27]. Therefore, it is meaningful to compare the spectrum of the W-shaped soliton and the Peregrine rw. We can analyze the spectrum evolution $F(\omega,z) = \frac{1}{\sqrt{2\pi}} \int_{-\infty}^{+\infty} E(t,z) \exp[-i\omega t]\, dt$ of the W-shaped soliton exactly though Fourier transformation. The background is infinity and thus its integral is $\delta(\omega - \omega_0)$ (here the background frequency is $\omega_0 = \frac{1}{6\epsilon}$), then we can eliminate the δ function and obtain the spectrum of the W-shaped soliton. For an example, the spectrum expression of the W-shaped soliton in Case 1 can be calculated as

$$|F(\omega,z)|^2 = 16\pi \exp\left(-\frac{|\omega'|}{\sqrt{2}}\right), \tag{5}$$

where $\omega' = \omega - \omega_0$. The spectrum evolution for the W-shaped soliton is illustrated in Fig. 5(a). Similarly, we can analyze the spectrum of the W-shaped soliton with other values of ω_0 exactly. We find that all spectrum evolutions are stable triangular spectrum. For comparison, we also give the spectrum of the Peregrine rw as [28]

$$|F_1(\omega,z)|^2 = 2\pi \exp(-|\omega|\sqrt{1+4z^2}). \tag{6}$$

The corresponding spectrum evolution is shown in Fig. 5(b). It is seen that the spectrum for the Peregrine rw is widely broadened near $z = 0$, which could be seen as a supercontinuum generation [26]. Notice that the profiles of the spectrum distribution of the W-shaped soliton and the rw at $z = 0$ are very similar and their temporal intensity distributions are identical at this position. This partly indicates that the W-shaped soliton corresponds to the supercontinuum generation. Moreover, the spectrum of the W-shaped soliton with other values of ω_1 also has triangular characters.

In particular, we further analyze the spectrum evolution of the rw solution in the S-S model [12,13], where the rw solution demonstrates two humps around one location and two eye-shaped rws can be observed. As an example, we choose the ones given in Eqs. (32)–(35) in Ref. [13] to discuss the spectrum characters. Here we replace the variables x and t with t and z, respectively. The explicit expressions of the spectrum $F_p(\omega,z)$ can be written as follows: For $\omega' > 0$, we have

$$F_p(\omega,z) = \frac{\sqrt{2\pi}i[G(t_2,z) + iH(t_2,z)]\ \exp[i\omega' t_2]}{(t_2 - t_1)(t_2 - t_3)(t_2 - t_4)} + \frac{\sqrt{2\pi}i[G(t_4,z) + iH(t_4,z)]\ \exp[i\omega' t_4]}{(t_4 - t_1)(t_4 - t_2)(t_4 - t_3)}, \tag{7}$$

while for $\omega' < 0$ we have

$$F_p(\omega,z) = \frac{\sqrt{2\pi}i[G(t_1,z) + iH(t_1,z)]\ \exp[i\omega' t_1]}{(t_1 - t_2)(t_1 - t_3)(t_1 - t_4)} + \frac{\sqrt{2\pi}i[G(t_3,z) + iH(t_3,z)]\ \exp[i\omega' t_3]}{(t_3 - t_1)(t_3 - t_2)(t_3 - t_4)}, \tag{8}$$

where $\omega' = \omega - \frac{k}{2\epsilon}$ ($-\frac{k}{2\epsilon}$ is the background frequency). t_2 and t_4 are the roots of $D(t,z) = 0$ on the upper half plane of complex, and t_1 and t_3 are the roots on the lower half plane. The explicit expressions for the functions $G(t,z)$, $H(t,z)$, and $D(t,z)$ are given by Eqs. (33)–(35) in Ref. [13], respectively. The spectral extension is around the center $\frac{k}{2\epsilon}$ frequency. The spectrum is not continuous at $\omega' = 0$, since there is a third power of t in the expression of $H(t,z)$ which is lower by one power than the highest power of t in $D(t,z)$. In Fig. 5(c), we only demonstrate the spectrum in the case of $k = 0.25$, $\epsilon = 0.5$, and $c = 1$, which corresponds to the spectrum evolution of the RW in Fig. 2 in Ref. [13]. Obviously, an interference pattern during the twisting process is observed, which shows quite a difference compared with the spectrum for the W-shaped soliton.

V. DISCUSSION AND CONCLUSION

We have presented an exact rational solution of the S-S equation, which can be used to describe the W-shaped soliton in a nonlinear fiber with higher-order effects such as higher-order dispersion, Kerr dispersion, and stimulated inelastic scattering. Interestingly, we have found that the height of the hump of the W-shaped soliton strongly depends on the frequency of the background field. In the regime $0 \leqslant \omega_1 \leqslant \frac{c}{2}$, the hump's height is found to be inversely proportional to the background frequency. The spectrum analysis suggests that the W-shaped soliton corresponds to a supercontinuum pulse, which may lead to extensively applications in frequency metrology, ultrafast science, imaging, flow cytometry, communications, and other areas [29–32]. Particularly, we have compared the spectrum of the W-shaped soliton, Peregrine rw, and the rw pair solution in the S-S model. For the Peregrine rw, the modulational instability induced supercontinuum generation has been demonstrated in Refs. [2,26,27] and the supercontinuum is unstable since the modulational instability mechanism. For the rw pair in Refs. [12,13], the spectrum is also unstable and there is an interference pattern emerging during the twisting process. However, our W-shaped soliton corresponding to the supercontinuum is stable, which has been checked by the numerical simulations with some small perturbations.

ACKNOWLEDGMENTS

We are grateful to Professor Zhan-Ying Yang and Dr. Kang Jin for their helpful discussions in revision process. This work is supported by the National Natural Science Foundation of China (Grants No. 11305120 and No. 11047025), the ministry of education doctoral program funds (Grant No. 20126101110004), and the Fundamental Research Funds for the Central Universities of China.

APPENDIX: THE EXPLICIT FORM OF THE RATIONAL SOLUTION

For $0 < \omega_1 \leqslant \frac{c}{2}$, the rational solution is

$$E(t,z) = c\left[1 - \frac{H(t,z)}{G(t,z)}\right]\exp\left[i\omega_0 t + iK(z)\right], \qquad \text{(A1)}$$

where $H(t,z)$ and $G(t,z)$ are

$$\begin{aligned}
H =\ & 12b(2b+m-3i\omega_1)^2\big(16b^2z\epsilon+4bmz\epsilon-2m^2z\epsilon-3T-9\omega_1^2z\epsilon-3\big)\big[32b^3z\epsilon+24b^2z\epsilon(m+2i\omega_1)\\
&-6b\big(-2im\omega_1z\epsilon+T+3\omega_1^2z\epsilon+1\big)-2m^3z\epsilon-6im^2\omega_1z\epsilon-3m\big(T+3\omega_1^2z\epsilon+1\big)-9i\big(T\omega_1+3\omega_1^3z\epsilon+\omega_1+i\big)\big],\\
G =\ & 4096z^2\epsilon^2b^8+10240mz^2\epsilon^2b^7+256z\epsilon\big(72z\epsilon c^2-6T+37m^2z\epsilon+54\omega_1^2z\epsilon-6\big)b^6+128mz\epsilon\left(216z\epsilon c^2-27T\right.\\
&\left.+26m^2z\epsilon+135\omega_1^2z\epsilon-27\right)b^5+16\big[-20z^2\epsilon^2m^4+108\omega_1^2z^2\epsilon^2m^2-180z\epsilon m^2+9T^2+81\omega_1^4z^2\epsilon^2-378\omega_1^2z\epsilon\\
&+216c^2z\epsilon\big(3z\epsilon m^2+6\omega_1^2z\epsilon-2\big)-18T\big(24z\epsilon c^2+10m^2z\epsilon+21\omega_1^2z\epsilon-1\big)+9\big]b^4-32\left\{16z^2\epsilon^2m^5+6z\epsilon\big(12z\epsilon c^2\right.\\
&\left.+5T+27\omega_1^2z\epsilon+5\big)m^3-9\left[-45z^2\epsilon^2\omega_1^4-24z\epsilon\omega_1^2+T^2-6c^2z\epsilon\big(3z\epsilon\omega_1^2+5\big)+T\big(-30z\epsilon c^2-24\omega_1^2z\epsilon+2\big)+1\right]m\right.\\
&\left.-324c^2z\epsilon\right\}b^3-8\left\{10z^2\epsilon^2m^6+216\omega_1^2z^2\epsilon^2m^4-27\left[-45z^2\epsilon^2\omega_1^4-6z\epsilon\omega_1^2+T^2+T\big(2-6\omega_1^2z\epsilon\big)+1\right]m^2\right.\\
&-27c^2\big[-8z^2\epsilon^2m^4-12z\epsilon\big(6z\epsilon\omega_1^2+1\big)m^2+36z\epsilon m+3T^2-189\omega_1^4z^2\epsilon^2-54\omega_1^2z\epsilon-6T\big(2z\epsilon m^2+9\omega_1^2z\epsilon-1\big)+3\big]\\
&\left.-81\omega_1^2\big[-27z^2\epsilon^2\omega_1^4-6z\epsilon\omega_1^2+T^2+T\big(2-6\omega_1^2z\epsilon\big)+1\big]\right\}b^2+8\left\{27\big[2z\epsilon\big(-3z\epsilon\omega_1^2+T+1\big)m^3\right.\\
&+3\big(-9z^2\epsilon^2\omega_1^4+T^2+2T+1\big)m-9\big(3z\epsilon\omega_1^2+T+1\big)\big]c^2+m\big(m^2+9\omega_1^2\big)\left[9T^2+9\big(z\epsilon m^2+3\omega_1^2z\epsilon+2\big)T\right.\\
&\left.\left.+(z\epsilon m^2+3)\big(2z\epsilon m^2+9\omega_1^2z\epsilon+3\big)\right]\right\}b+\big(m^2+9\omega_1^2\big)^2\big(2z\epsilon m^2+3T+9\omega_1^2z\epsilon+3\big)^2\\
&+18c^2\left\{4z^2\epsilon^2m^6+12z\epsilon\big(6z\epsilon\omega_1^2+T+1\big)m^4-36z\epsilon m^3+9\left[45z^2\epsilon^2\omega_1^4+18z\epsilon\omega_1^2+T^2+2T\big(9z\epsilon\omega_1^2+1\big)+1\right]m^2\right.\\
&\left.-54\big(3z\epsilon\omega_1^2+T+1\big)m+81\big[9z^2\epsilon^2\omega_1^6+6(T+1)z\epsilon\omega_1^4+(T+1)^2\omega_1^2+1\big]\right\},
\end{aligned}$$

with $T = t - \frac{z}{12\epsilon}$, $\omega_1 = \omega_0 - \frac{1}{6\epsilon}$, $m = \sqrt{4b^2-6c^2-3\omega_1^2}$, and $b = \sqrt{[c^4-\sqrt{c^2(c^2-4\omega_1^2)^3}]/\omega_1^2+10c^2-2\omega_1^2}/2\sqrt{2}$.

For $\omega_1 = 0$, the rational solution is

$$E(t,z) = -\frac{c[576c^6z^2\epsilon^2-96c^4(T+1)z\epsilon+24\sqrt{2}c^3z\epsilon+4c^2(T+1)^2-2\sqrt{2}c(T+1)-1]}{576c^6z^2\epsilon^2-96c^4(T+1)z\epsilon+24\sqrt{2}c^3z\epsilon+4c^2(T+1)^2-2\sqrt{2}c(T+1)+1}\exp\left[i\frac{t}{6\epsilon}-i\frac{z}{108\epsilon^2}\right]. \qquad \text{(A2)}$$

[1] B. Kibler, J. Fatome, C. Finot, G. Millot, F. Dias, G. Genty, N. Akhmediev, and J. M. Dudley, Nat. Phys. **6**, 790 (2010).
[2] J. M. Dudley, G. Genty, F. Dias, B. Kibler, and N. Akhmediev, Opt. Express **17**, 21497 (2009).
[3] B. Kibler, J. Fatome, C. Finot *et al.*, Sci. Rep. **2**, 463 (2012).
[4] K. Porsezian and K. Nakkeeran, Phys. Rev. Lett. **76**, 3955 (1996).
[5] Y. Kodama and A. Hasegawa, IEEE J. Quantum Electron. **23**, 510 (1987).
[6] N. Sasa and J. Satsuma, J. Phys. Soc. Jpn. **60**, 409 (1991).
[7] O. C. Wright, III, Chaos Solitons Fractals **33**, 374 (2007).
[8] Z. H. Li, Lu Li, H. P. Tian, and G. S. Zhou, Phys. Rev. Lett. **84**, 4096 (2000).
[9] D. Mihalache, L. Torner, F. Moldoveanu, N.-C. Panoiu, and N. Truta, J. Phys. A **26**, L757 (1993).
[10] D. Mihalache, N.-C. Panoiu, F. Moldoveanu, and D.-M. Baboiu, J. Phys. A **27**, 6177 (1994).
[11] D. Mihalache, L. Torner, F. Moldoveanu, N.-C. Panoiu, and N. Truta, Phys. Rev. E **48**, 4699 (1993).
[12] U. Bandelow and N. Akhmediev, Phys. Rev. E **86**, 026606 (2012).
[13] S. H. Chen, Phys. Rev. E **88**, 023202 (2013).
[14] V. Ruban, Y. Kodama, M. Ruderman *et al.*, Eur. Phys. J.: Spec. Top. **185**, 5 (2010).
[15] N. Akhmediev and E. Pelinovsky, Eur. Phys. J.: Spec. Top. **185**, 1 (2010).
[16] C. Kharif and E. Pelinovsky, Eur. J. Mech. B: Fluids **22**, 603 (2003).
[17] E. Pelinovsky and C. Kharif, *Extreme Ocean Waves* (Springer, Berlin, 2008).
[18] M. Gedalin, T. C. Scott, and Y. B. Band, Phys. Rev. Lett. **78**, 448 (1997).
[19] C. Gilson, J. Hietarinta, J. Nimmo, and Y. Ohta, Phys. Rev. E **68**, 016614 (2003).

[20] J. Kim, Q.-Han Park, and H. J. Shin, Phys. Rev. E **58**, 6746 (1998).
[21] K. Nakkeeran, K. Porsezian, P. S. Sundaram, and A. Mahalingam, Phys. Rev. Lett. **80**, 1425 (1998).
[22] J. S. He, H. R. Zhang, L. H. Wang, K. Porsezian, and A. S. Fokas, Phys. Rev. E **87**, 052914 (2013).
[23] Y. Ohta and J. K. Yang, Proc. R. Soc. London, Ser. A **468**, 1716 (2012).
[24] B. L. Guo, L. M. Ling, and Q. P. Liu, Phys. Rev. E **85**, 026607 (2012).
[25] Z. J. Qiao, J. Math. Phys. **48**, 082701 (2007); **47**, 112701 (2006).
[26] D. R. Solli, C. Ropers, and B. Jalali, Phys. Rev. Lett. **101**, 233902 (2008).
[27] D. R. Solli, B. Jalali, and C. Ropers, Phys. Rev. Lett. **105**, 233902 (2010).
[28] N. Akhmediev, A. Ankiewicz, J. M. Soto-Crespo, and J. M. Dudley, Phys. Lett. A **375**, 541 (2011).
[29] J. M. Dudley, G. Genty, and S. Coen, Rev. Mod. Phys. **78**, 1135 (2006).
[30] S. A. Diddams, L. Hollberg, and V. Mbele, Nature (London) **445**, 627 (2007).
[31] D. Wildanger, E. Rittweger, L. Kastrup, and S. W. Hell, Opt. Express **16**, 9614 (2008).
[32] V. Kapoor, F. V. Subach, V. G. Kozlov *et al*., Nat. Methods **4**, 678 (2007).